PERGAMON

International Journal of Solids and Structures 38 (2001) 2131–2147

INTERNATIONAL JOURNAL OF SOLIDS and STRUCTURES

www.elsevier.com/locate/ijsolstr

Methods for dimension reduction and their application in nonlinear dynamics

Alois Steindl, Hans Troger *

Institut für Mechanik, Technische Universität Wien, Wiedner Hauptstrasse 8-10/325, A-1040 Wien, Austria

Received 27 July 1999; in revised form 7 December 1999

Abstract

We compare linear and nonlinear Galerkin methods in their efficiency to reduce infinite dimensional systems, described by partial differential equations, to low dimensional systems of ordinary differential equations, both concerning the effort in their application and the accuracy of the resulting reduced system.

Important questions like the choice of the form of the ansatz functions (modes), the choice of the number m of modes and, finally, the construction of the reduced system are addressed. For the latter point, both the linear or standard Galerkin method making use of the Karhunen Loeve (proper orthogonal decomposition) ansatz functions and the nonlinear Galerkin method, using approximate inertial manifold theory, are used. In addition, also the post-processing Galerkin method is compared with the other approaches.

Keywords: Nonlinear dynamics; Dimension reduction; Galerkin methods

1. Introduction

In the field of engineering, the description of a dynamical system is usually given by a differential equation

$$\dot{\boldsymbol{v}} = \boldsymbol{G}(\boldsymbol{v}, \lambda), \tag{1}$$

where, in the general case, $\boldsymbol{v}$ is an element of a Hilbert space $\boldsymbol{E}$, and $\boldsymbol{G}(\boldsymbol{v}, \lambda)$ is a smooth nonlinear operator. As an example, we treat in Section 4 a fluid conveying tube. In that, the control parameter λ corresponds to the flow rate.

Eq. (1) defines a time continuous dynamical system given by the mapping

$$\boldsymbol{v}(t) = \varphi_t(\boldsymbol{v}_0) = \varphi(t; \boldsymbol{v}_0, t_0), \tag{2}$$

where $\boldsymbol{v}(t)$ is the current state of the system, and $\varphi(t; \boldsymbol{v}_0, t_0)$ is the solution of the differential equation (1) for the given initial data $\boldsymbol{v}_0$ at t_0. The‘ariable $\boldsymbol{v}$ can be a point in an infinite or finite dimensional phase space (Troger and Steindl, 1991). The mapping (2) defines a flow (the time evolution) in phase space.

* Corresponding author. Fax: +43-1-588-0132598.
E-mail address: hans.troger@tuwien.ac.at (H. Troger).

0020-7683/01/$ - see front matter
PII: S0020-7683(00)00157-8

A finite dimensional phase space of high dimension or an infinite dimensional phase space, as it is obtained for the fluid conveying tube, will create great difficulties in analyzing the dynamics both qualitatively and quantitatively. Hence, one always will try to reduce the system's dimension – if this can be done at all – and to achieve a good approximation of the original dynamics. This goal can be reached for certain dissipative systems, basically by neglecting inessential degrees of freedom of the system. That this should be possible is indicated both by experiments and engineering experience. It is well known that the asymptotic behavior of high dimensional or even infinite dimensional dissipative dynamical systems can often be described by the deterministic (possibly chaotic) flow on a low dimensional attractor A. In addition, there exists also a number of mathematical model equations for which this property has been proven to hold rigorously (Rodriguez and Sirovich, 1990; Bloch and Titi, 1990; Jones et al., 1995).

Now, let us explain the dimension reduction of a dynamic system from our understanding. We restrict to one of the central problems in stability theory, namely the investigation of loss of stability of an equilibrium $\boldsymbol{v}_e$ of Eq. (1) under quasi-static variation of a distinguished system parameter λ (Troger and Steindl, 1991). First, we rewrite Eq. (1) in the form

$$\dot{\boldsymbol{u}} = \boldsymbol{L}(\lambda)\boldsymbol{u} + \boldsymbol{g}(\boldsymbol{u}, \lambda), \tag{3}$$

where $\boldsymbol{L} = \boldsymbol{G}_v(\boldsymbol{v}_e)$ is the linearization of the operator $\boldsymbol{G}$ at the equilibrium position $\boldsymbol{v}_e, \boldsymbol{g}$ is a smooth nonlinear operator and $\boldsymbol{u} = \boldsymbol{v} - \boldsymbol{v}_e$ is the deviation from $\boldsymbol{v}_e$. Both the operators $\boldsymbol{L}$ and $\boldsymbol{g}$ are still dependent on the spatial variable $\boldsymbol{x}$. In addition, we assume that $\boldsymbol{g}(\boldsymbol{0}, \lambda) = \boldsymbol{0}$ and $\boldsymbol{g}_u(\boldsymbol{0}, \lambda) = \boldsymbol{0}$. Basically, the loss of stability is described in terms of the temporal evolution of the amplitudes of certain (active) modes, the determination of which is the key point in dimension reduction. These modes, roughly speaking, are those that are either mildly unstable or only slightly damped in linear theory. For their determination, in general, an eigenvalue problem following from the linearized part of Eq. (3) must be solved. If the number of these critical modes is finite, a set of ordinary differential equations can be constructed, which governs the evolution of their amplitudes. These equations are called *amplitude equations of the critical modes or bifurcation equations*, and they basically describe the behavior of the original system, since the other (possibly infinitely many) modes are more or less strongly damped and, hence, do not explicitly appear in the description (Coullet and Spiegel, 1983). This scenario can also be given a geometric interpretation in phase space. The evolution of the flow basically can be split into two parts. One, which is rapidly decaying towards an attracting manifold and this is, as center manifold theory shows, due to the negative real parts of the corresponding eigenvalues of the linearization of this part of the flow. The second part of the flow, which for the long term behavior of the system is the essential one, evolves slowly on the attracting manifold, since, in general, it is dominated by nonlinear terms, because the corresponding eigenvalues of its linearization are located close to the imaginary axis. This picture comes out clearly from the center manifold theory as depicted in Fig. 1 in the frames (a)–(c) for the loss of stability at a zero eigenvalue described by the simple system

$$\dot{q} = qp, \quad \dot{p} = -p + aq^2 \tag{4}$$

and in frame (d) for the loss of stability at a purely imaginary eigenvalue for a Hopf bifurcation in a three-dimensional phase space (see also Section 2). Basically, we can conclude that the two-dimensional system (4) may be reduced to a one-dimensional one which evolves on the center manifold. However, though intuitively quite plausible, it would be a mistake to assume that the fast motion, which corresponds to the higher modes in the representation of the system, can be completely ignored in the derivation of the reduced system. Due to nonlinear coupling, the elimination of the fast motion (higher modes) is a delicate matter. If the fast motion is completely ignored in the calculation of the reduced system, the so-called standard (linear or flat) Galerkin method, mostly used in engineering, is obtained. However, we will show that better strategies exist. In some sense, the representation of the higher modes by means of the lower modes is the essential step in applying more sophisticated dimension reduction methods.

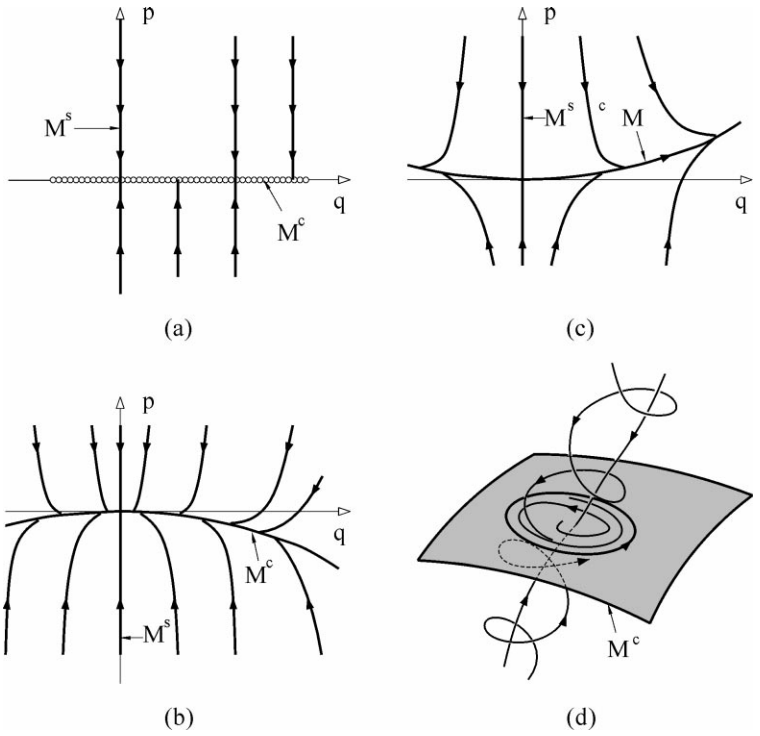

Fig. 1. Center manifolds and flows: (a) for the linear part of system (4), (b) and (c) for the nonlinear system (4) for $a < 0$ and $a > 0$, respectively and (d) for a three-dimensional system after a Hopf bifurcation.

Hence, in general, we want to derive from Eq. (3), a finite dimensional system of the form

$$\frac{\mathrm{d}\boldsymbol{q}}{\mathrm{d}t} = \boldsymbol{f}(\boldsymbol{q}, \lambda), \quad \boldsymbol{q} \in \mathbb{R}^m. \tag{5}$$

The solution of Eq. (5) should allow to approximate the field $\boldsymbol{u}(\boldsymbol{x}, t)$, for example, in the form (12) in some proper norm. The $q_i(t)$ are the amplitudes of the active modes, and Eq. (5) are the amplitude equations describing their time evolution. The main difficulties in providing the link between Eqs. (3) and (5) are

1. identifying the spatial structure of the active modes,
2. determining the number of active modes,
3. selecting a method to construct the reduced system (5).

It is difficult if not impossible to give answers to these questions in general. However, if we restrict to the scenario of loss of stability of an equilibrium, then quite precise answers can be given (Aceves et al., 1986). We assume that for a range of parameter values of λ, Eq. (3) has an asymptotically stable equilibrium position $\boldsymbol{u}_\mathrm{e} = \boldsymbol{0}$. Now, we vary λ quasi-statically and assume that for $\lambda = \lambda_\mathrm{c}$, a loss of stability of u_e occurs. If this scenario applies, then in two cases a proper dimension reduction may be performed ($\varepsilon \ll 1$):

1. If $|\lambda - \lambda_\mathrm{c}| = \mathcal{O}(\varepsilon)$, the *center manifold theory* may be applied.
2. If $|\lambda - \lambda_\mathrm{c}| = \mathcal{O}(1)$, *Galerkin methods* may be useful.

Case 1 is well studied in books on bifurcation theory (Carr, 1981; Guckenheimer and Holmes, 1983; Troger and Steindl, 1991) and, for example, in the papers Holmes (1981), Coullet and Spiegel (1983), well accessible for engineers. Provided an additional condition, which is stated below, holds, a precise identification of the form and the number of the active modes exists. If Case 2 applies, we want to compare several alternatives to the *standard Galerkin method*, usually used by engineers. Here, the literature is more challenging mathematically, but well written papers are by Bloch and Titi (1990), Brown et al. (1990), Brunovsky (1993), Jones et al. (1995) and Garcia-Archilla et al. (1998).

Though we will concentrate on *Galerkin methods*, we start with a short review of *center manifold theory* because it most clearly displays what dimension reduction is all about.

2. Center manifold theory

For $|\lambda - \lambda_c| = \mathcal{O}(\varepsilon)$ and some additional requirements (Troger and Steindl, 1991), where the most important is that at the critical parameter value $\lambda = \lambda_c$, the eigenvalue with largest real part, crossing the imaginary axis, has finite multiplicity (n_c) center manifold theory is applicable. Then, the field variable $\boldsymbol{u}(\boldsymbol{x}, t)$ is decomposed in the form

$$\boldsymbol{u}(\boldsymbol{x}, t) = \boldsymbol{u}_c(\boldsymbol{x}, t) + \boldsymbol{u}_s(\boldsymbol{x}, t) = \sum_{i=1}^{n_c} q_i(t)\chi_i(\boldsymbol{x}) + \boldsymbol{U}(q_i(t), \boldsymbol{x}), \tag{6}$$

where the $\chi_i(\boldsymbol{x})$ are the active spatial modes, obtained from the solution of the eigenvalue problem related to the linear system

$$\dot{\boldsymbol{u}} = \boldsymbol{L}(\lambda_c)\boldsymbol{u}. \tag{7}$$

The $q_i(t)$ are their time-dependent amplitudes and $\boldsymbol{u}_s(\boldsymbol{x}, t)$ could be given by an infinite sum. The key point is that the influence of the infinite number of higher modes contained in $\boldsymbol{u}_s(\boldsymbol{x}, t)$ can be expressed in terms of the lower order modes by the function $\boldsymbol{U}(q_i(t), \boldsymbol{x})$.

We indicate now, how Eq. (5) is obtained from Eq. (3). We assume that the spectrum of $\boldsymbol{L}(\lambda)$ is discrete and that for $\lambda = \lambda_c$, a finite number (n_c) of eigenvalues crosses the imaginary axis at the same time. All other eigenvalues have a negative real part. Now, we rewrite Eq. (3) in the form

$$\dot{\boldsymbol{u}}_c = P\boldsymbol{L}\boldsymbol{u}_c + P\boldsymbol{g}(\boldsymbol{u}_c + \boldsymbol{u}_s), \tag{8a}$$

$$\dot{\boldsymbol{u}}_s = Q\boldsymbol{L}\boldsymbol{u}_s + Q\boldsymbol{g}(\boldsymbol{u}_c + \boldsymbol{u}_s), \tag{8b}$$

by decomposing $\boldsymbol{E} = \boldsymbol{E}_c \oplus \boldsymbol{E}_s$, where $\boldsymbol{E}_c$ is finite (n_c) dimensional and $\boldsymbol{E}_s$ is closed (we recall that a space $\boldsymbol{E}$ is closed if any Cauchy sequence $\boldsymbol{u}_v$ for $v \to \infty$ possesses a limit $\boldsymbol{u}$ in $\boldsymbol{E}$). This decomposition is achieved by defining the projection P (see Troger and Steindl (1991)) onto $\boldsymbol{E}_c$ along $\boldsymbol{E}_s$, giving $\boldsymbol{u}_c = P\boldsymbol{u} \in \boldsymbol{E}_c$ and $\boldsymbol{u}_s = Q\boldsymbol{u} \in \boldsymbol{E}_s$ where $Q = I - P$. If $\boldsymbol{u}_s = \boldsymbol{h}(\boldsymbol{u}_c)$ is a smooth invariant manifold (a manifold M is invariant, if for every initial value $\boldsymbol{u}_0 \in M$ the trajectory $\varphi_t(\boldsymbol{u}_0)$ remains in M for all $t \geqslant 0$), we call $\boldsymbol{h}$ a center manifold if $\boldsymbol{h}(\boldsymbol{0}) = \boldsymbol{h}'(\boldsymbol{0}) = \boldsymbol{0}$. Note, that if in Eqs. (8a) and (8b) $P\boldsymbol{g} = Q\boldsymbol{g} = \boldsymbol{0}$, all solutions tend exponentially fast to solutions of $\dot{\boldsymbol{u}}_c = P\boldsymbol{L}\boldsymbol{u}_c$ (see Fig. 1, frame (a)). That is, the linear n_c dimensional equation on the (flat) center manifold determines the asymptotic behavior of the entire infinite dimensional linear system, up to exponentially decaying terms. The center manifold theorem enables us to extend this argument to the nonlinear case when $P\boldsymbol{g}$ and $Q\boldsymbol{g}$ are not equal to zero.

Center manifold theorem (Carr, 1981). (1) *There exists a center manifold* $\boldsymbol{u}_s = \boldsymbol{h}(\boldsymbol{u}_c)$ *for system* (8), *if* $|\boldsymbol{u}_c|$ *is sufficiently small. The behavior of system* (8) *on the center manifold is governed by the equation*

$$\dot{\boldsymbol{u}}_c = P\boldsymbol{L}\boldsymbol{u}_c + P\boldsymbol{g}(\boldsymbol{u}_c + \boldsymbol{h}(\boldsymbol{u}_c)). \tag{9}$$

(2) *The zero solution of Eqs.* (8) *has exactly the same stability properties as the zero solution of Eq.* (9).
(3) *If* $\boldsymbol{H} : R^{n_c} \to R^{n_s}$ *is a smooth map with* $\boldsymbol{H}(\boldsymbol{0}) = \boldsymbol{H}'(\boldsymbol{0}) = \boldsymbol{0}$ *and is defined by the equation* (3.25) *in Troger and Steindl* (1991)

$$\boldsymbol{P}(\boldsymbol{H}) := \boldsymbol{H}'(\boldsymbol{u}_c)[P\boldsymbol{L}\boldsymbol{u}_c + P\boldsymbol{g}(\boldsymbol{u}_c + \boldsymbol{H}(\boldsymbol{u}_c))] - Q\boldsymbol{L}\boldsymbol{H}(\boldsymbol{u}_c) - Q\boldsymbol{g}(\boldsymbol{u}_c + \boldsymbol{H}(\boldsymbol{u}_c)), \tag{10}$$

then if

$$\boldsymbol{P}(\boldsymbol{H}) = \mathcal{O}(|\boldsymbol{u}_c|^r), \quad r > 1 \text{ as } |\boldsymbol{u}_c| \to 0,$$

we have $|\boldsymbol{h}(\boldsymbol{u}_c) - \boldsymbol{H}(\boldsymbol{u}_c)| = \mathcal{O}(|\boldsymbol{u}_c|^r)$ as $|\boldsymbol{u}_c| \to 0$.

We note that by inserting $\boldsymbol{u}_s = \boldsymbol{h}(\boldsymbol{u}_c)$ into Eqs. (8), we can eliminate the (infinitely many) inessential variables $\boldsymbol{u}_s$ to obtain Eq. (9) which is a system of n_c nonlinear ordinary differential equations for the n_c amplitudes $q_i(t)$ of the active modes $\chi_i(\boldsymbol{x})$. Moreover, Eq. (9) describes the whole nearby (local) dynamics of the original infinite dimensional system (3) together with Eq. (6). We further remark that the $\boldsymbol{u}_s$ in Eq. (6) are at least of second order in $\boldsymbol{u}_c$, that is

$$\boldsymbol{u}_s = \mathcal{O}(||\boldsymbol{u}_c||^2) = \mathcal{O}(|q_i|^2). \tag{11}$$

Relation (11) has important consequences concerning the practical calculations (Troger and Steindl, 1991). Part 3 of the theorem allows to calculate a sufficiently accurate approximation by retaining relevant terms in a Taylor series expansion.

3. Galerkin approximation

Often in technical problems the case of a small parameter variation ($|\lambda - \lambda_c| = \mathcal{O}(\varepsilon)$), as it is required for *center manifold theory*, is not valid because deviations ($|\lambda - \lambda_c| = \mathcal{O}(1)$) about λ_c occur or many eigenvalues are located close to but not exactly on the imaginary axis. In the latter case, variation of the parameter λ beyond the critical value λ_c will have the effect that additional modes become unstable and, hence, the originally low dimensional system will not be valid anymore. For such problems, Galerkin methods may be used.

In general, applying Galerkin methods (Meirovitch, 1967), the field variable $\boldsymbol{u}(\boldsymbol{x}, t)$ is expressed in the form

$$\boldsymbol{u}(\boldsymbol{x}, t) = \sum_{j=1}^{m} q_j(t)\psi_j(\boldsymbol{x}) \tag{12}$$

by a set of m comparison vectors (functions) $\psi_j(\boldsymbol{x})$, called the Galerkin basis, which must satisfy all the geometric and natural boundary conditions.

In engineering notation, applying the standard Galerkin method means that Eq. (3) is projected on the space of ansatz functions ψ_j in the form

$$\left(\left[\frac{\mathrm{d}}{\mathrm{d}t} - \boldsymbol{L} - \boldsymbol{g} \right] \left(\sum_{j=1}^{m} q_j(t)\psi_j(x) \right), \psi_j(\boldsymbol{x}) \right) = 0 \tag{13}$$

which results in the amplitude equations

$$\dot{q}_j = f_j^m(q_1, \ldots, q_m), \quad j = 1, \ldots, m. \tag{14}$$

The inner product in Eq. (13) is nothing else than the projection P used in Eq. (8). Besides the choice of $\psi_j(\boldsymbol{x})$, a major open question in the application of the standard Galerkin approximation is the proper choice of m. Whereas the dimension n_c of the *center manifold* is determined by the number of eigenvalues of the linear operator $\boldsymbol{L}$ which, at the first time, cross the vertical axis at the critical parameter value λ_c, and hence, is precisely known, there does not exist such a precise and sharp criterion which would allow to fix m in the Galerkin approximation. One always will try to select m as small as possible in order to make further treatment of the system (14) of nonlinear ordinary differential equations for the $q_j(t)$ as simple as possible. However, the number m must be chosen large enough to catch the qualitative behavior of the problem. That is, beyond a certain value of m an increase of the number m should not have any influence on the qualitative behavior of the phenomenon. For a discussion of this point in relation to the Lorenz equations, derived from the Bénard convection problem, see Aceves et al. (1986), where it is shown that the increase of m beyond $m = 3$ results in qualitative changes in the dynamics of the truncated system (see also Saltzman (1962)).

Applying the Galerkin methods, engineers usually use the standard Galerkin approximations for the reduction of the dimension of the problem. However, besides the standard Galerkin method, nonlinear Galerkin methods (see also Section 3.2.1) are also available. The difference between standard and nonlinear Galerkin can be best understood from our short presentation of center manifold theory considering Eqs. (6) and (8). Standard Galerkin means that one neglects $\boldsymbol{u}_s$ in Eq. (6), and consequently, only Eq. (8a) is obtained, with $\boldsymbol{u}_s = 0$ inserted into the nonlinear function $P\boldsymbol{g}$. Hence, the fast dynamics expressed by the function $\boldsymbol{U}(q_i(t), \boldsymbol{x})$ in Eq. (6) and taken care of in center manifold theory is completely ignored in the reduction process of the system. We note that for system (4) this would yield a completely useless result. Nonlinear Galerkin means that the influence of the higher modes $\boldsymbol{u}_s$ is not neglected as in the standard Galerkin reduction. To take care of the influence of $\boldsymbol{u}_s$ in Eq. (8a), several possibilities exist. Two possibilities are explained below.

To handle the three difficulties raised in the Introduction, one can choose between several possibilities:

1. For the standard Galerkin reduction, instead of the usual choice of ansatz functions (Meirovitch, 1967) as comparison functions, the Karhunen Loeve method could be used to obtain a set of optimal ansatz functions. Here, optimal means that for the same m, the Karhunen Loeve ansatz functions supply a better approximation than any other choice of ansatz functions (Holmes et al., 1996). Moreover, the Karhunen Loeve method allows to formulate an energy estimate, which supplies important information concerning the number m of active modes to be retained in the approximate system, to achieve a certain accuracy.

2. The standard Galerkin method can be extended to the so-called nonlinear Galerkin methods which in the mathematical literature are better known as the concept of inertial manifolds. Here, we include two possibilities for the practical calculations:

(a) approximate inertial manifold theory,
(b) post-processed Galerkin method.

3.1. Karhunen Loeve method

Here, we only make some general remarks concerning the Karhunen Loeve method (Lumley, 1970), because a detailed presentation in engineering style is given in Steindl et al. (1999).

The Karhunen Loeve method, which in the mathematical literature (Sirovich, 1987; Holmes et al., 1996) is called proper orthogonal decomposition method, has been quite successfully applied for the study of turbulence and coherent structures in fluid flow problems. Basically, it requires the availability of an ensemble of data functions u_i, which may be generated from experiments or numerical simulations. From this data, one wants to find a deterministic function f which in some statistical sense has the structure typical of

the members u_i of the ensemble. Let us assume that u is a vector in a function space. Then f should be as nearly parallel as possible to u in a statistical sense. We assume that the projection of u on f given by (u,f) is defined. The task is to maximize (u,f). Obviously, one can increase the value of (u,f) simply by increasing the magnitude of f without changing its form. Hence, one must normalize by the length of the vector f. This results in the quantity

$$\frac{(u,f)}{(f,f)^{1/2}} \tag{15}$$

which has to be maximized on a Hilbert space of functions f, where (f,f) exists. Since we have a whole ensemble of functions u_i, we have to maximize in some average sense. If the mean value of the u_i is zero one would obtain $E\{(u,f)\}=0$, where $E\{\cdot\}$ denotes the ensemble average (Steindl et al., 1999). Hence, instead of Eq. (15), the quadratic expression

$$\frac{E\{(u,f),(u,f)\}}{(f,f)} \geqslant 0, \tag{16}$$

is maximized. It is shown in Holmes et al. (1996) (Section 3.1) that Eq. (16) is equivalent to the constrained minimum problem: extremalize $E\{(u,f)^2\}$ with $(f,f)=1$.

This is a standard problem in the calculus of variations and results in an eigenvalue problem of the form

$$(R(x,x'),\phi(x')) = \int_D R(x,x'),\phi(x')\,\mathrm{d}x' = \lambda\phi(x). \tag{17}$$

The generalized function $R(x,x')=E\{u(x)u(x')\}$ is the covariance or the autocorrelation of $u(x)$ and $u(x')$ where $u(x)$ is a regular function absolutely integrable on the finite region D. The solution of Eq. (17) supplies the set of optimal eigenmodes ϕ_j. Another interpretation of optimality is that the mean square error between the approximate and the exact solution is a minimum for the KL-basis at any truncation point (Steindl et al., 1999). The corresponding eigenvalues λ_j can be interpreted as a measure of the energy content carried by the corresponding mode. If they are normalized as probabilities, their sum gives the percentage of energy represented by the approximation.

Finally, we note that, if $R(x,x')=R(x-x')$, then the $\phi_j(x)$ are given by $\phi_j(x)=e^{ijx}$, that is, by trigonometric functions. Moreover, for the optimal eigenfunctions or eigenvectors, a geometric interpretation is possible, because they approximate the data in such a way that they are parallel to the axis of the inertia ellipsoid of the cloud of data points. In this respect, mathematically, besides the statistical aspect, a problem is given, completely analogous to the calculation of the principal moments of inertia of a body in $\mathbb{R}^3$ (Parkus, 1966, Section 2.5). Applications of the Karhunen Loeve method are given in Steindl et al. (1999).

3.2. Nonlinear Galerkin method: inertial manifold

Often a strong improvement of the quality of the approximation is achieved if instead of the traditional standard Galerkin method, use of nonlinear Galerkin methods is made and here as mathematical concept inertial manifolds are used (Brunovsky, 1993; Guckenheimer, 1989; Marion and Temam, 1989). An inertial manifold is a finite dimensional, exponentially attracting manifold. The qualitative idea is that if a system possesses a complicated attractor A, then it can often be better approximated by a nonlinear manifold as given by the inertial manifold than by the linear space used in the standard Galerkin method. Again, restricting the infinite dimensional system to such a manifold yields a finite dimensional system of ordinary differential equations, which approximates the long-term dynamics of the original system. The proof that such inertial manifolds exist has been given for a variety of partial differential equations (Brunovsky, 1993). An intuitively easily understood condition for the existence of such inertial manifolds (Guckenheimer, 1989) is the requirement that the separation of trajectories within the manifold must be less extreme than in

the direction transversal to the manifold. This condition results in requirements on spectral gaps for the linearized operator $\boldsymbol{L}$ in Eq. (3). In other words, the attracting invariant manifold must have more extreme Ljapunov exponents in its normal directions than in its tangential directions. If the partial differential equations being studied have large gaps in their spectrum, then these can be used to look for invariant manifolds that are located close to the linear space spanned by the modes corresponding to the eigenvalues which are located to the right of a gap in the complex plane. For realistic examples, the main problem, in looking for such a gap condition, is that the estimates on the dimension m of the inertial manifold obtained in the literature (Bloch and Titi, 1990; Brunovsky, 1993; Jones et al., 1995) are very large and practically useless, since, in general, only very low dimensional systems can be fully analyzed concerning their qualitative behavior.

3.2.1. Approximate inertial manifold

Here, we follow engineering requirements and give a brief description on how, by treating a problem, an approximation of an inertial manifold can be calculated. We proceed similarly as in the center manifold reduction and follow Foias et al. (1988). We start with system (3). We order the real parts of the eigenvalues of the linear operator $\boldsymbol{L}$ by $\mu_1 \geqslant \mu_2 \geqslant \cdots$ Further, as before, we denote the projections onto the span of the first m eigenfunctions of $\boldsymbol{L}$ by P and on the orthogonal complement by $Q = I - P$. Then, Eqs. (8a) and (8b) is obtained exactly (with $n_c = m$). The traditional standard Galerkin approximation of Eq. (3) would proceed in the following way. From the eigenfunctions of $\boldsymbol{L}$, one selects the m modes and completely ignores Eq. (8b) and sets $\boldsymbol{u}_s = 0$ in Eq. (8a). This results in

$$\dot{\boldsymbol{u}}_{ml} = P\boldsymbol{L}\boldsymbol{u}_{ml} + P\boldsymbol{g}(\boldsymbol{u}_{ml}), \tag{18}$$

where the index l stands for linear. This would mean that the influence of the fast dynamics on the slow (essential) dynamics is completely neglected. However, sometimes a much better approximation is achieved if we make the assumption that Eq. (3) has an inertial manifold of dimension m which can be realized as the graph of a function $\boldsymbol{h} : P\boldsymbol{E} \to Q\boldsymbol{E}$ or in other words, $\boldsymbol{u}_s = \boldsymbol{h}(\boldsymbol{u}_{mn})$. The projection of the inertial form onto $P\boldsymbol{E}$ is then given by

$$\dot{\boldsymbol{u}}_{mn} = P\boldsymbol{L}\boldsymbol{u}_{mn} + P\boldsymbol{g}(\boldsymbol{u}_{mn} + \boldsymbol{h}(\boldsymbol{u}_{mn})), \tag{19}$$

where the index n stands for nonlinear. Now the approximation of $\boldsymbol{u}$ is given by

$$\boldsymbol{u}_{\text{app}} = \boldsymbol{u}_{mn} + \boldsymbol{h}(\boldsymbol{u}_{mn}), \tag{20}$$

completely analogous to Eq. (6). The interpretation of Eq. (20) is that the high frequency modes are expressed as a function of the low frequency modes.

Eq. (19) looks identical to Eq. (9) but in the practical calculations the following approach has to be taken. First, one makes a standard Galerkin approximation (18) with n modes. Then, one calculates an m-dimensional approximation ϕ of the inertial manifold $\boldsymbol{h}$ with $m < nv$, which is assumed to exist. Such an approximation of the inertial manifold can be calculated by an iterative scheme proposed in Brown et al. (1990). We designate the m critical variables by $\boldsymbol{q} \subset \mathbb{R}^m$ and the noncritical variables by $p \subset \mathbb{R}^{n-m}$ and rewrite the nth order system (18) in the following form:

$$\frac{\mathrm{d}\boldsymbol{q}}{\mathrm{d}t} = \mathbf{A}\boldsymbol{q} + P\boldsymbol{g}(\boldsymbol{q} + \boldsymbol{p}), \tag{21a}$$

$$\frac{\mathrm{d}\boldsymbol{p}}{\mathrm{d}t} = \mathbf{B}\boldsymbol{p} + Q\boldsymbol{g}(\boldsymbol{q} + \boldsymbol{p}). \tag{21b}$$

Here, $\mathbf{A} = P\boldsymbol{L}$ and $\mathbf{B} = Q\boldsymbol{L}$ where $P : \mathbb{R}^n \to \mathbb{R}^m$ denotes the projection to the m modes and $Q = I - P$ is the projection onto the orthogonal complement spanned by the eigenfunctions corresponding to the eigen-

values $\mu_{m+1},\ldots,\mu_n$. For the selection of the critical modes corresponding to the matrix $\mathbf{A}$ we look at the spectrum of the linear operator of the n-dimensional system. One usually picks those with the largest real parts that are located in a close neighborhood of the imaginary axis of the complex plane with the additional condition (hopefully satisfied) that they are well separated by a gap from all other eigenvalues, corresponding to the matrix $\mathbf{B}$, which are located further to the left in the complex plane. However, we will show in Section 4 that this approach sometimes may yield bad results. We now replace Eqs. (21a) and (21b) by

$$\frac{\mathrm{d}\boldsymbol{q}}{\mathrm{d}t} = \mathbf{A}\boldsymbol{q} + P\boldsymbol{g}(\boldsymbol{q} + \phi_{\mathrm{a}}(\boldsymbol{q})), \tag{22}$$

where ϕ_{a} is an approximation of the inertial manifold. In calculating the approximation, we note that close to the manifold $\mathrm{d}\boldsymbol{p}/\mathrm{d}t$ in Eq. (21b) is approximately zero. Hence, by setting $\mathrm{d}\boldsymbol{p}/\mathrm{d}t = \mathbf{0}$, we obtain the nonlinear equation

$$\mathbf{0} = \mathbf{B}\boldsymbol{p} + Q\boldsymbol{g}(\boldsymbol{q} + \boldsymbol{p}) \tag{23}$$

for $\boldsymbol{p}$, which may be solved by iterating the map

$$T(\boldsymbol{p}) = -\mathbf{B}^{-1}Q\boldsymbol{g}(\boldsymbol{q} + \boldsymbol{p}). \tag{24}$$

The approximate inertial manifold ϕ is given as its fixed point. The iteration may be started with $\phi_0 \equiv 0$, which is the linear approximation used in the traditional standard Galerkin approach. Then, the first two iterates yield

$$\phi_1 = -\mathbf{B}^{-1}Q\boldsymbol{g}(\boldsymbol{q}), \quad \phi_2 = -\mathbf{B}^{-1}Q\boldsymbol{g}(\boldsymbol{q} + \phi_1(\boldsymbol{q})), \ldots \tag{25}$$

However, we note that due to the neglect of $\dot{\boldsymbol{p}}$ in Eq. (24), it does not make sense to calculate higher approximations. This can be shown by comparisons with center manifold theory, performed for simple examples in Steindl et al. (1997). These comparisons show that already at low orders, qualitative discrepancies can occur.

The efficiency of the nonlinear Galerkin approach is demonstrated in Foias et al. (1988) for a reaction diffusion equation which is treated in two different ways: first, by the standard Galerkin approximation with $m = n = 3$ and, second, by a nonlinear Galerkin approximation starting with $n = 6$ and the assumption that a three-dimensional inertial manifold $m = 3$ exists. The results are compared with those obtained by a numerical bifurcation analysis performed for the discretized system with $m = 16$. It is shown that the Galerkin-inertial manifold approximation with $n = 6$ and reducing to $m = 3$ gives both qualitatively and quantitatively much better results than the standard Galerkin approximation with $m = 3$.

3.2.2. Post-processed Galerkin method

The main disadvantage in the application of the nonlinear Galerkin method in comparison with the standard Galerkin method is that more complicated calculations have to be performed. Naturally, the question arises whether this extra cost is worth for the enhancement of accuracy achieved. In particular, not only ϕ_{a} must be computed at every step in the integration of Eq. (22) but also the integration of Eq. (22) is more costly, than the integration of Eq. (22) where ϕ_{a} is set identical to zero. Hence, as an alternative, the post-processed Galerkin method has been proposed quite recently, for example, in Garcia-Archilla et al. (1998). It is shown in Laing et al. (1999) to be a method which incorporates the higher accuracy of the nonlinear Galerkin method at lower computational costs. In its application, first, the standard Galerkin method is used and only at time (t) when some output is required, the variables are lifted up to the approximation of the inertial manifold. That is, starting from Eq. (22) setting $\phi_a = \phi_1 = 0$, the solution $\boldsymbol{q}_m = \boldsymbol{q}_{ml}$ is calculated from

$$\frac{\mathrm{d}\boldsymbol{q}_{ml}}{\mathrm{d}t} = \mathbf{A}\boldsymbol{q}_{ml} + P\boldsymbol{g}(\boldsymbol{q}_{ml}). \tag{26}$$

This certainly can be done with less effort than calculating $\boldsymbol{q}_m = \boldsymbol{q}_{ma}$ from Eq. (22) given by

$$\frac{\mathrm{d}\boldsymbol{q}_{ma}}{\mathrm{d}t} = \mathbf{A}\boldsymbol{q}_{ma} + P\boldsymbol{g}(\boldsymbol{q}_{ma} + \phi_1(\boldsymbol{q}_{ma})). \tag{27}$$

However, $\boldsymbol{q}_{ml}$ calculated from Eq. (26) will in general be less accurate than $\boldsymbol{q}_{ma}$ calculated from Eq. (27). In order to increase the accuracy of $\boldsymbol{q}_{ml}$, it is now post-processed or in other words, lifted up to the approximate inertial manifold given by ϕ_1 from Eq. (25) at time t. This results in the solution $\boldsymbol{u}_{\mathrm{pp}}$ in the form

$$\boldsymbol{u}_{\mathrm{pp}}(t) \approx \boldsymbol{q}_{ml}(t) + \phi_1(\boldsymbol{q}_{ml}(t)). \tag{28}$$

Whereas $\boldsymbol{u}_{\mathrm{aim}}$, the solution of the more complicated system (27) is given by

$$\boldsymbol{u}_{\mathrm{aim}}(t) \approx \boldsymbol{q}_{ma}(t) + \phi_1(\boldsymbol{q}_{ma}(t)). \tag{29}$$

In Garcia-Archilla et al. (1998), for specific equations, error estimates are given concerning the accuracy of the various approximations. It is shown that the post-processed solution $\boldsymbol{u}_{\mathrm{pp}}$ is often as accurate as the approximate inertial manifold $\boldsymbol{u}_{\mathrm{aim}}$ solution.

However, computationally a great reduction in effort is achieved, since lifting of the solution of Eq. (26) onto the approximate inertial manifold needs to be done only when output is required, rather then at every time step as in the integration of Eq. (27).

4. Comparison of various methods for the large amplitude oscillations of a fluid conveying tube

To compare the various methods for an engineering problem, we study the self-excited large amplitude oscillations of the fluid conveying tube depicted in Fig. 2. The tube is clamped at its upper end, free at its lower end and is restricted to perform planar oscillations. The description of the mechanical model and the derivation of the equations of motion is given in Steindl and Troger (1996). For the planar motion of the tube, the displacement u_1 in the direction of x_1 is introduced (Fig. 2). In order to find the critical flow rate ϱ_c, the linearized eigenvalue problem

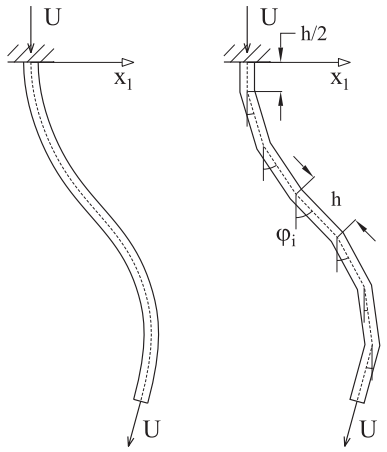

Fig. 2. Continuous and discrete model of a fluid conveying tube: $\varrho \approx U$ is the nondimensional flow rate.

$$\ddot{u}_1 + \alpha_e \dot{u}_1 + u_1^{iv} + \alpha_1 \dot{u}_1^{iv} + 2\sqrt{\beta}\varrho \dot{u}_1'' + \varrho^2 u_1'' - \gamma[(1-s)u_1']' = 0 \tag{30}$$

with the boundary conditions

$$u_1(0) = u_1'(0) = 0,$$

$$u_1''(1) + \alpha_1 \dot{u}_1'' = u_1'''(1) + \alpha_1 \dot{u}_1''' = 0,$$

which corresponds to system (7), must be solved. For the data given in Sugiyama et al. (1985) at $\varrho = \varrho_c \approx 8.027$, a loss of stability of the downhanging tube by a supercritical Hopf bifurcation occurs (Steindl and Troger, 1992).

Following Steindl (1997), we compare three different ways to select ansatz functions for the Galerkin reduction:

1. Eigenvectors of the linearized problem at $\varrho_s = 10.0 > \varrho_c \approx 8.027$. The eigenvectors are sorted according to the value of the real part of the corresponding eigenvalue. The location of the eigenvalues is depicted in Fig. 3. At $-1/\alpha_1 \approx -50$, where α_1 is the material damping coefficient, an accumulation of the eigenvalues is clearly visible.
2. Oscillation modes of a clamped tube (beam). The mode shapes of the unloaded undamped tube (without fluid) are sorted according to their node number.
3. Karhunen Loeve basis. The data necessary for the KL-analysis is obtained by simulating the motion of the tube for $\varrho_s = 10.0$.

The simulations have been performed by a finite difference discretization with $N = 32$ elements for data taken from Sugiyama et al. (1985). This results in a $n = 64$ dimensional system. Some tube shapes resulting from these simulations are shown in Fig. 4. Though the value of ϱ_s is not much larger than ϱ_c, a large amplitude motion is setting in.

Fig. 5 displays simulation results depicting the projection of the limit cycle on the $(\varphi_{16}, \dot{\varphi}_{16})$ plane. Results calculated with the $n = 64$ dimensional system designated by (+) are compared with those obtained

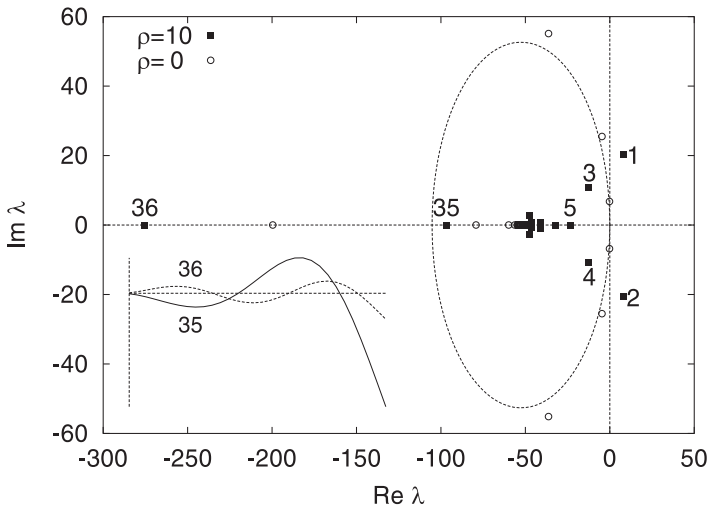

Fig. 3. Distribution of the eigenvalues in the complex plane for $\varrho = 0$ and $\varrho = \varrho_s$ and the modes shapes corresponding to the eigenvalues numbered 35 and 36.

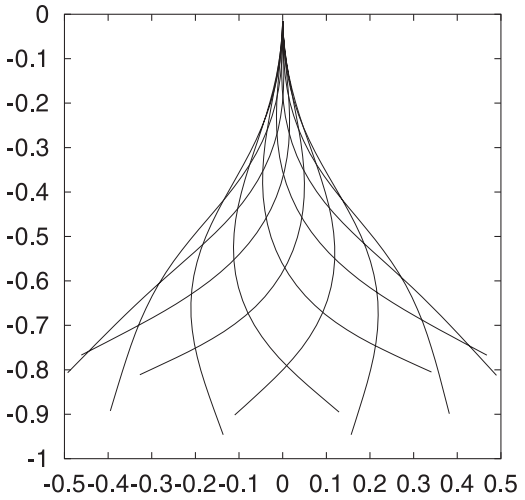

Fig. 4. Simulation of the fluid conveying tube for $\varrho_s = 10$. A finite difference discretization with $N = 32$ elements is used, resulting in a system with dimension $n = 64$.

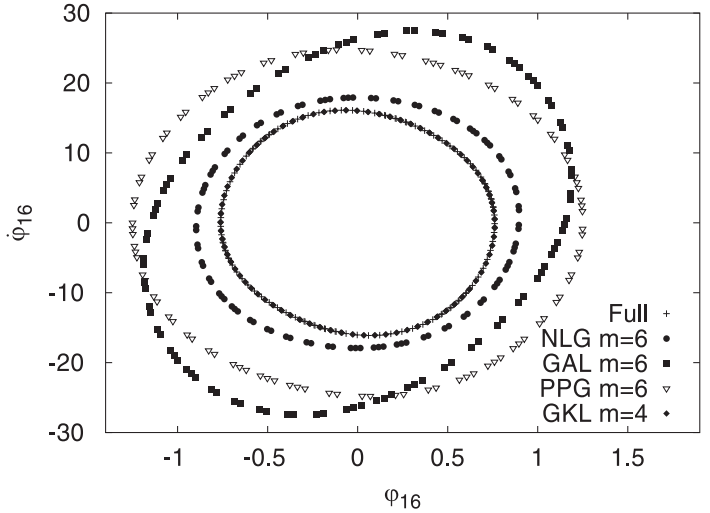

Fig. 5. Projection of the simulation results on the $(\varphi_{16}, \dot{\varphi}_{16})$ plane for full system $n = 64$ ("Full"), standard Galerkin ("GAL"), nonlinear Galerkin ("NLG"), Galerkin with KL modes ("GKL") and post-processed Galerkin ("PPG"). The results for Full and GKL are not distinguishable.

from the simulation with three six-dimensional and one four-dimensional systems. These are the standard Galerkin ("GAL"), with six modes, the nonlinear Galerkin ("NLG") where starting from the 64 modes, by means of the approximate inertial manifold, the 58 passive modes have been expressed by the six active modes, the post-processed Galerkin ("PPG") where the results of standard Galerkin are lifted to the approximation of the inertial manifold and the standard Galerkin with four KL ansatz functions ("GKL") Obviously, the ranking is GKL, NLG, PPG and GAL. For the three latter methods (NLG, PPG and GAL) as ansatz functions, the eigenmodes of the linearized problem have been used.

In order to see which modes (eigenvectors) make relevant contributions to the motion of the tube, we consider the limit cycle designated by (+) in Fig. 5. It is obtained from simulating the full 64-dimensional system. The accuracy of the various Galerkin approximations is clearly visible. The inner most limit cycle is the "exact" solution. Basically, an identical result is obtained from the standard Galerkin using Karhunen Loeve ansatz functions (GKL) with $m = 4$. The next in accuracy is nonlinear Galerkin (NLG) with $m = 6$. Then follow post-processed Galerkin (PPG) and standard Galerkin (GAL). In order to gain more insight, we ask now for the average contribution $\bar{a}_k$ of the kth mode (eigenvector) in the limit cycle which is given by

$$\bar{a}_k^2 = \frac{1}{J}\sum_{i=1}^{J} a_k^2(t_i).$$

Here, $J = 200$ is used. For the three different choices of modes, the results are shown in Fig. 6 for the eigenvector basis, in Fig. 7 for the beam eigenvectors, and in Fig. 8 for the Karhunen Loeve eigenvectors. In all these figures, $\bar{a}_k$ is drawn versus the corresponding mode.

Obviously, there are strong qualitative differences. Whereas for the beam eigenvectors (Fig. 7) and for the Karhunen Loeve eigenvectors (Fig. 8), the contribution of the higher modes decays monotonically, this is not the case for the eigenvectors obtained from the solution of the linearized fluid conveying tube problem (Fig. 6). From Fig. 6, it is clearly visible that there are eigenvectors (e.g. 35 and 36) located further left in the complex plane, where they are marked in Fig. 3, which contribute more than some located closer to the imaginary axis. In order to give an explanation of this, at the first moment *v* surprising fact *v*, we consider the way how the eigenvalues are located in the complex plane (Fig. 3). To be able to calculate the distribution of the eigenvalues analytically we restrict to the tube without fluid, but for the fluid carrying tube a similar situation holds qualitatively. From Eq. (30) follows

$$\ddot{u}_1 + u_1^{iv} + \alpha_1 \dot{u}_1^{iv} = 0, \tag{31}$$

where the influence of gravity is also neglected. The boundary conditions are the same as for Eq. (30). Setting $u_1(s,t) = \exp(\lambda t)x(s)$ and $\mu^4 = -\lambda^2/(1+\alpha_1\lambda)$, we obtain the eigenvalue problem for the clamped–free beam. The graph shown in Fig. 9 explains the structure of the eigenvalues. Basically, there exists three different sets of eigenvalues. First, the set of complex eigenvalues (μ_1, μ_2) approximately located on a circle

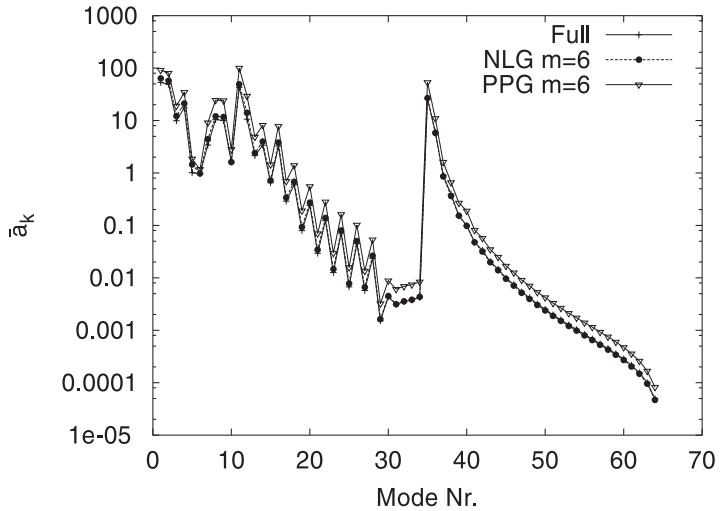

Fig. 6. Averaged contribution of each of the first 64 eigenvectors (modes) to the limit cycle oscillation.

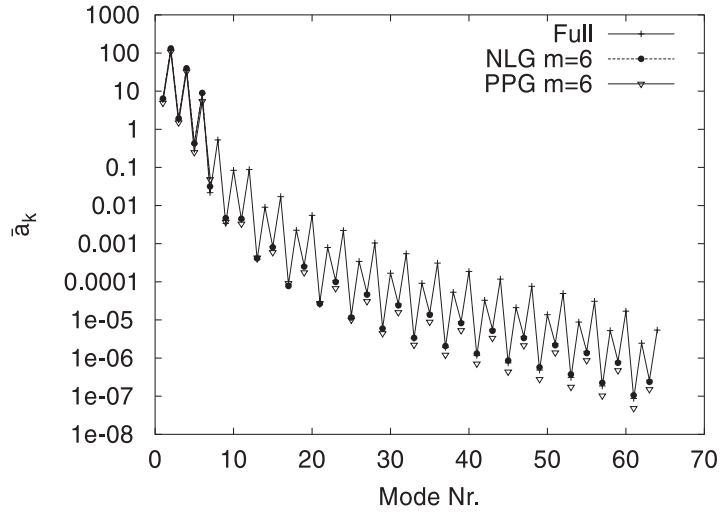

Fig. 7. Averaged contribution of the first 64 beam modes to the limit cycle oscillation.

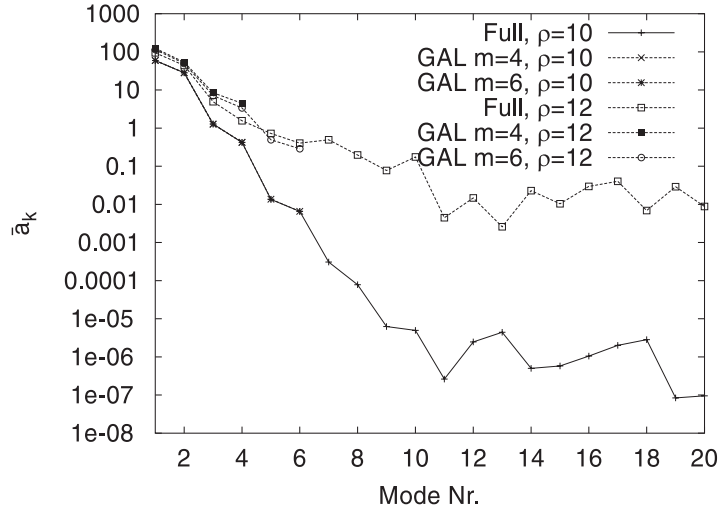

Fig. 8. Averaged contribution of the KL modes to the limit cycle oscillation. The results for $\varrho = 12$ are calculated from the simulation data obtained with $\varrho = 10$.

of radius $-1/\alpha_1$ centered at the point close to $-1/\alpha_1$. This point is an accumulation point to which the second set converges. Finally, the third set is the family of eigenvalues converging rapidly to $-\infty$. These latter two sets contain real eigenvalues. Now, it is easy to understand that the numbering of the eigenvalues according to the amount of the real part is not a natural one, since those located close to the approximate circle and located left to the accumulation point have lower node numbers, than those converging to the accumulation point. This is shown in Fig. 3 where the shapes of the modes number 35 and 36 are depicted. They have two and three nodes, respectively, whereas, for example, the modes number 30 and 31 have seven and eight nodes, respectively. Hence, this confirms the statement made before that in such cases the choice

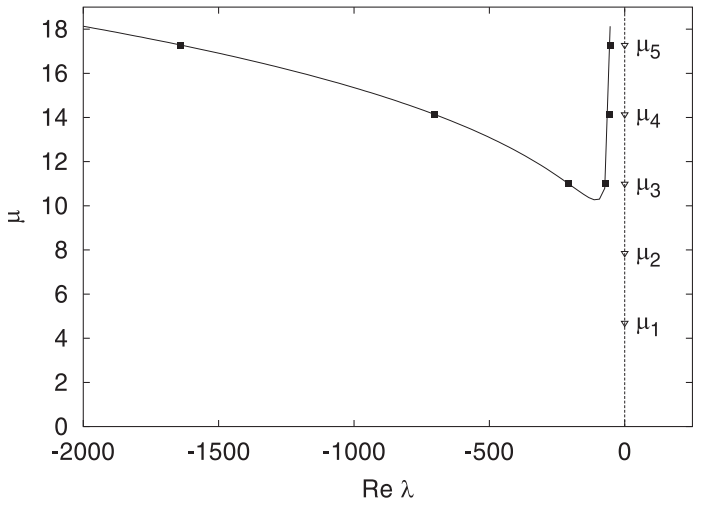

Fig. 9. Eigenvalues μ_i of the beam equation (31). For $\mu = \mu_1$ and $\mu = \mu_2$, the corresponding eigenvalues λ are complex valued.

of the ansatz modes taking into account the amount of the real part of the corresponding eigenvalues may result in inaccurate results.

The zig-zag curve in Fig. 7 results from the fact that the upper points correspond to velocity modes and the lower points to position modes.

From Fig. 8 and Table 1, an important feature of the KL-approximation can be recognized. As already mentioned, the normalized eigenvalues of the KL-approximation given in Table 1, represent the fraction of the energy of the various modes. Obviously, for these eigenfunctions, a very good approximation is already achieved for a small number of modes (two) for the standard Galerkin approximation. Nevertheless, it was necessary to include four modes, as depicted in Fig. 10, in the approximation because with only two modes (one degree of freedom) no flutter instability, but a divergent instability was obtained, which is a meaningless result. The KL-calculation is performed from 1000 data points taken from the simulation at equidistant intervals of Δt. However, we also note from Fig. 8 that the claim made in the literature that with a reduced system formed with KL ansatz functions obtained at one parameter value ϱ_1 simulations also can be performed for a range of parameter values $\varrho \neq \varrho_1$ has to be considered with caution even if the same bifurcation pattern is found. In case the bifurcation pattern changes, no good results are to be expected. In such a case, simulation of the original system in a range of parameter values would be necessary, where

Table 1
Normalized eigenvalues of the KL reduction representing the energy contribution of the respective mode

$n = 4$	$n = 8$	$n = 16$	$n = 32$	$n = 64$
0.7661	0.8049	0.8128	0.8138	0.8147
0.2073	0.1936	0.1867	0.1857	0.1848
0.0265	0.0012	4.64E−4	3.97E−4	3.80E−4
2.2E−5	1.86E−4	5.93E−5	4.49E−5	4.15E−5
	1.66E−7	8.76E−8	4.98E−8	4.30E−8
	1.84E−9	2.26E−8	1.17E−8	9.96E−9
	...	...	...	...

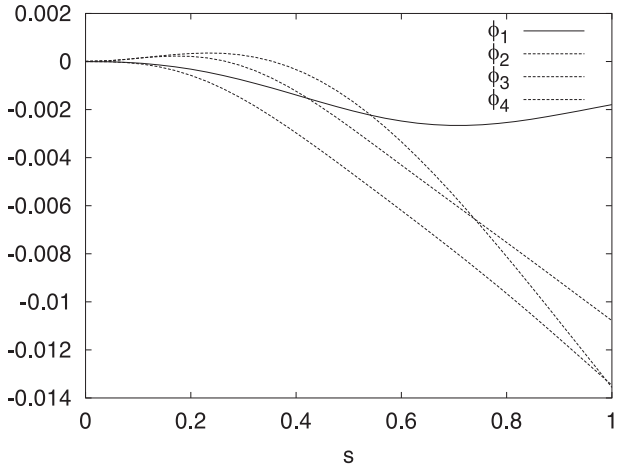

Fig. 10. Shapes of the first two KL modes.

different types of motions are present to generate more general data, from which the KL-modes could be calculated. One possibility could also be to simulate the system in the chaotic regime.

5. Conclusion

Among the different sets of ansatz functions, the KL modes are by far the best choice for a standard Galerkin approximation, because the contribution of the higher modes decays most rapidly.

For an arbitrary choice of ansatz functions, the nonlinear Galerkin method certainly is superior to the standard Galerkin method. This is especially important if the dimension of the reduced system is chosen to be very small, which always will be the goal of a reduction process, because only for a low dimensional system a reasonable qualitative analysis can be performed. That the results of the KL approximation for the tube oscillations are so good could be a consequence that the limit cycle, from which the data is sampled, can be very well approximated by a low dimensional linear space. Although only two modes make an essential contribution to the energy content, it was still necessary to include four ansatz modes, because with two modes no reasonable approximation for the original dynamics was obtained. With the post-processed Galerkin method only a slight increase in accuracy was achieved for this example.

Concerning the computational efforts the calculation of the KL modes requires, first, the generation of simulation data and the solution of an eigenvalue problem. Then, however, only a standard Galerkin reduction with a very low number of modes is necessary. For the nonlinear Galerkin method the ansatz functions are usually given. In the case that the eigenfunctions of the linearized problem are used they are obtained from the calculation of the stability problem. However, for the nonlinear Galerkin reduction the calculation of the reduced system is at least twice as expensive as for the standard Galerkin method. On the other hand, post-processing may be performed following a standard Galerkin reduction at very low additional computational costs.

Finally, we remark that using the eigenmodes of the linearized problem as ansatz functions can lead to problems as described in Section 5. The reason is that the introduction of internal damping due to the Kelvin–Voigt law of linear visco-elasticity, an accumulation point in the spectrum occurs. This has the consequence that the eigenvalues with smaller node number have a larger real part than eigenvalues with a larger node number.

Acknowledgements

This research project has been supported by the Austrian Science Foundation (FWF), under the project P 13131-MAT. We also would like to thank the referees for their valuable comments.

References

Aceves, A., Adachihara, H., Jones, C., Lerman, J.C., McLaughlin, D.W., Moloney, J.V., Newell, A.C., 1986. Chaos and coherent structures in partial differential equations. Physica D 18, 85–112.

Bloch, A.M., Titi, E.S., 1990. On the dynamics of rotating elastic beams. New Trends in Systems Theory. Birkhäuser, Boston, pp. 128–135.

Brown, H.S., Jolly, M.S., Kevrekidis, I.G., Titi, E.S., 1990. Use of approximate inertial manifolds in bifurcation calculations. In: Roose, D., et al. (Eds.), Continuation and Bifurcations: Numerical Techniques and Applications, Kluwer Academic Publishers, Dordrecht, pp. 9–23.

Brunovsky, P., 1993. Theory of invariant manifolds and its applications to differential equations. UTMS 93-41, Dept. Math. Sci., University of Tokyo.

Carr, J., 1981. Applications of centre manifold theory. Applied Math. Sciences, vol. 35, Springer, New York.

Coullet, P.H., Spiegel, A., 1983. Amplitude equations for systems with competing instabilities. SIAM J. Appl. Math. 43, 776–821.

Foias, C., Jolly, M.S., Kevrekidis, I.G., Sell, G.R., Titi, E.S., 1988. On the computation of inertial manifolds. Phys. Lett. A 131, 433–437.

Garcia-Archilla, B., Novo, J., Titi, E.S., 1998. Postprocessing the Galerkin method: a novel approach to approximate inertial manifolds. SIAM J. Numer. Anal. 35 (3), 941–972.

Guckenheimer, J., 1989. Infinite-dimensional dynamical systems in mechanics and physics. In: Temam, R. (Ed.), Bulletin of the AMS, vol. 21, pp. 196–198.

Guckenheimer, J., Holmes, P., 1983. Nonlinear oscillations, dynamical systems, and bifurcations of vector fields. Applied Math. Sciences, vol. 42, Springer, New York.

Holmes, P.J., 1981. Center manifolds, normal forms and vectorfields with application to coupling between periodic and steady motions. Physica 2D, 449–481.

Holmes, P., Lumley, J.L., Berkooz, G., 1996. Turbulence, Coherent Structures, Dynamical Systems and Symmetry. Cambridge University Press, New York.

Jones, D.A., Margolin, L.G., Titi, E.S., 1995. On the effectiveness of the approximate inertial manifold – a computational study. Theoret. Comput. Fluid Dynam. 7, 243–260.

Laing, C.R., McRobie, A., Sell, G.R., Thompson, J.M.T., 1999. The post-processed Galerkin method applied to nonlinear shell vibrations. Dynamics and Stability of Systems 14, 163–181.

Lumley, J.L., 1970. Stochastic Tools in Turbulence. Academic Press, New York.

Marion, M., Temam, R., 1989. Nonlinear Galerkin methods. SIAM J. Numer. Anal. 26, 1139–1157.

Meirovitch, L., 1967. Analytical Methods in Vibrations. Macmillan, New York.

Parkus, H., 1966. Mechanik fester Körper. Springer, New York.

Rodriguez, J.D., Sirovich, L., 1990. Low-dimensional dynamics for the complex Ginzburg–Landau equation. Physica D 43, 77–86.

Saltzman, B., 1962. Finite amplitude free convection as an initial value problem – I. J. Atmosph. Sci. 19, 329–341.

Sirovich, L., 1987. Turbulence and the dynamics of coherent structures. Part I: Coherent structures; Part II: Symmetries and transformations; Part III: Dynamics and scaling. Quater. Appl. Math. XLV, 561–590.

Steindl, A., 1997. Dimension reduction methods for a fluid conveying tube. ZAMM 77, S321–S322.

Steindl, A., Troger, H., 1992. One- and two-parameter bifurcations to divergence and flutter in the three-dimensional motions of a fluid conveying viscoelastic tube with D_4-symmetry. Nonlinear Dynam. 8, 161–178.

Steindl, A., Troger, H., 1996. Equations of motion of a fluid conveying tube. In: Kirchgässner, K., Mahrenholtz, O., Mennicken, R. (Eds.), ICIAM 95, Math. Res., vol. 87, Akademie-Verlag, Berlin, pp. 533–536.

Steindl, A., Troger, H., Zemann, V., 1997. Nonlinear Galerkin methods applied in the dimension reduction of vibrating fluid conveying tubes, AD-Vol. 53-1, Book No. H1102A, ASME Publications, pp. 273–280.

Steindl, A., Troger, H., Zemann, V. 1999. Improved Galerkin methods for the dimension reduction of nonlinear dynamical systems. In: Moon, F.C. (Ed.), Proceedings of the IUTAM Symposium on New Applications of Nonlinear and Chaotic Dynamics in Mechanics, Kluwer Academic Publishers, Dordrecht, pp. 71–80.

Sugiyama, Y., Tanaka, Y., Kishi, T., Kawagoe, T., 1985. Effect of a spring support on the stability of pipes conveying fluid. J. Sound Vibra. 100, 257–270.

Troger, H., Steindl, A., 1991. Nonlinear Stability and Bifurcation Theory, An Introduction for Engineers and Applied Scientists. Springer, New York.